

# Effect of Soil Aging on Assessing Magnitudes and Accelerations of Prehistoric Earthquakes

Evangelia Leon,<sup>a)</sup> Sarah L. Gassman,<sup>b)</sup> and Pradeep Talwani<sup>c)</sup>

Increase in strength due to aging of sands is reflected in higher blow counts and tip resistance values in penetration resistance measurements. This affects the magnitudes and peak ground acceleration estimates of prehistoric earthquakes obtained from an analysis of geotechnical observations at paleoliquefaction sites in the South Carolina Coastal Plain. In this study, corrections were made to account for the effects of soil aging, which were neglected in earlier estimates. The results show that when the effects of aging of soils on their geotechnical properties are incorporated, the resulting back-calculations reduced earlier magnitude estimates of prehistoric earthquakes by about 0.9 units. The peak ground acceleration estimates were reduced by about 15% for those earthquakes originally estimated at approximately 0.15 g. For those earthquakes whose original estimates were greater than 0.2 g, there was no noticeable change when a correction was made for the aging of soils.

[DOI: 10.1193/1.1949223]

## INTRODUCTION

Paleoseismicity, the history of prehistoric earthquakes, is being used increasingly in seismic hazard analyses (SHA). In the western United States, where faults are exposed, the effects of prehistoric earthquakes can be directly studied in suitably placed trenches. In the eastern United States, large earthquakes are less frequent and in the absence of surficial evidence, the indirect effects of prehistoric earthquakes, such as sand blows embedded in soft sediments, are studied. By dating trapped organic material and, in some cases, associated archeological artifacts in and around sand blows, it has now become possible to reconstruct the chronology of past earthquakes associated with liquefaction (e.g., Talwani and Schaeffer 2001, Tuttle et al. 2002). This chronology of past earthquakes is used to infer the recurrence rate of large earthquakes, one of the parameters needed in SHA. Until recently, another parameter needed in SHA, the magnitudes of prehistoric earthquakes, was estimated indirectly. The magnitude of the prehistoric or paleoearthquake was based on the distribution of associated sand blows.

In the Charleston, South Carolina, region, the results of extensive paleoseismological investigations have revealed evidence of seven prehistoric earthquakes in the past 6,000 years (Table 1). Based on the more recent events, these data suggested that, on average,

---

<sup>a)</sup> Florence & Hutcheson, Inc., 2700 Middleburg Drive, Suite 150, Columbia, SC 29204; lleon@flohut.com

<sup>b)</sup> University of South Carolina, Department of Civil & Environmental Engineering, Columbia, SC 29208; gassman@enr.sc.edu

<sup>c)</sup> University of South Carolina, Department of Geological Sciences, Columbia, SC 29208; talwani@geol.sc.edu

**Table 1.** Paleoearthquake ages and associated sand blows in the SCCP (after Talwani and Schaeffer [2001] and Hu et al. [2002b])

Liquefaction Episode	Age, Years B.P.	Source	Associated Sand Blow	Re or R (km)
A	546±17	Charleston	SAM-02	100–140
B	1021±30	Charleston	SAM-04	100–140
C	1648±74	Northeast	SAM-05	10–35
C'	1683±70	Charleston	SAM-05	100–140
D	1966±212	South	...	...
E	3548±66	Charleston	GAP-02	100–140
F	5038±166	Northeast	GAP-03	10–35
F'	5038±166	Charleston	GAP-03	100–140
?		Charleston	TMHA	10–35
?		Charleston	TMHB	10–35

liquefaction causing earthquakes occurred every 500 years in the South Carolina Coastal Plain (SCCP) (see Talwani and Schaeffer [2001] for a review). Estimating the magnitudes of these prehistoric events, however, has been problematic. Talwani and Schaeffer (2001) compared the spatial extent of several prehistoric liquefaction features with the observed distribution of those associated with the M7.3 1886 Charleston earthquake to estimate these magnitudes. Earthquakes centered near Charleston were assigned magnitudes of 7+, and those located in northern (episodes C and F) and southern (episode D) source zones were assigned a magnitude of approximately 6. The magnitudes of these earthquakes were also estimated based on the epicentral distance to the farthest associated sand blow, using the magnitude-bound method established by Ambraseys (1988). This method gave magnitude estimates of approximately 7.0 for the prehistoric earthquakes centered at Charleston. Details regarding the estimates of distances and calculation of magnitudes are presented in Talwani and Schaeffer (2001).

Observations of liquefaction features about 100 km from the Loma Prieta earthquake of 1989, and their absence at shorter distances, suggested that site specific soil and water table conditions played an important role in the onset of liquefaction. Several studies have related various geotechnical parameters to earthquake magnitudes and peak ground accelerations needed for the onset of earthquake-induced liquefaction (e.g., Seed et al. 1985, Ishihara 1985, Ambraseys 1988, Martin and Clough 1994, Pond and Martin 1997, Seed et al. 2001, Idriss and Boulanger 2004). For this study, geotechnical observations (SPT blow count  $[(N_1)_{60}]$ , CPT tip resistance  $[q_{c1}]$ , and shear wave velocity  $[V_{s1}]$ ) were available at four locations in the vicinity of paleoliquefaction features found in the SCCP. Two sites were in Georgetown County at Sampit (SAM) and Gapway (GAP), and two sites were near Ten Mile Hill (TMHA and TMHB), north of the Charleston Air Force Base. These in-situ data were first analyzed by Hu et al. (2002a, b) to back-calculate the magnitudes and peak ground accelerations of the associated paleoearthquakes. The results suggested higher magnitudes for the prehistoric earthquakes than had been obtained empirically using the magnitude bound method. The empirical

methods used to back-calculate the magnitudes of the prehistoric earthquakes were based on data from Holocene soils, whereas the soils at the liquefaction sites in Georgetown County and Ten Mile Hill were about 450,000 and 200,000 years old. Therefore the work presented in this paper addresses the need to account for changes in the geotechnical properties (and the effect on the liquefaction threshold) that may have occurred because of age.

Increase in strength and stiffness of sand with time, a phenomenon known as aging, has been reported by Mitchell and Solymar (1984), Dowding and Hryciw (1986), Skempton (1986), Schmertmann (1987), and Mesri et al. (1990). The nature of the responsible mechanisms that cause aging continues to be uncertain, however, the most dominant aspects relate soil aging to mechanical and/or chemical factors. The responsible mechanisms that cause this phenomenon tend to increase the penetration resistance of the sand deposits as reflected in higher blow counts or tip resistance (Mitchell and Solymar 1984, Skempton 1986, Kulhawy and Mayne 1990). Large increases in the penetration resistance have also been observed following the use of ground modification techniques (Mitchell 1986, Schmertmann 1987, Mesri et al. 1990) such as vibrocompaction and blast densification. In paleoliquefaction evaluation the phenomenon of aging must be accounted for when examining the change in soil properties in a specified period of time between the occurrence of liquefaction and in-situ verification testing.

The objective of this study is to account for the effect of soil aging when estimating the magnitudes and induced peak ground accelerations of seven prehistoric earthquakes that produced paleoliquefaction features in the SCCP. To this end a geotechnical approach similar to the one followed by Hu et al. (2002b) was adopted, but instead of using the current resistance of the soil as expressed by the in-situ soil indices (SPT, CPT,  $V_s$ ), the resistance of the soil before the occurrence of the earthquake was used. Quantitative correlations that comprise the effect of aging on in-situ soil indices were used to estimate the resistance of the soil prior to the earthquake. The geotechnical data are corrected for aging of the soil over time, as well as the disturbance due to liquefaction event. The corrected geotechnical data are used to represent the soil conditions at the sites prior to the prehistoric earthquake to assess the earthquake magnitude and induced peak ground acceleration.

## SOIL AGING

### PROPOSED MECHANISMS FOR AGING OF SANDS

Research conducted during the last two decades to investigate the different mechanisms that cause aging in sands has generally focused on mechanical and chemical mechanisms. Mechanical mechanisms involve macro-interlocking of sand particles, micro-interlocking of surface roughness, and internal stress arching, which occur during secondary consolidation. Chemical mechanisms involve dissolution and precipitation of silica or other soluble material like carbonate minerals. Youd and Hoose (1977) were among the earliest investigators to provide an explanation on the increased resistance of sands with age. They reported that the potential mechanism to explain the reduction in

liquefaction susceptibility with age was the cementing and compaction of the soil by natural processes, as well as changes in topography, water table depth, and depth of burial due to postdepositional geologic processes.

More specific explanations for the increase in strength of sand due to aging were later proposed by Mitchell and Solymar (1984) and Mitchell (1986). They suggested that aging of sands as measured by resistance to penetration over periods up to several months is a result of chemical mechanisms. More recently, evidence supporting this mechanism was presented by Joshi et al. (1995). They conducted a series of lab tests with an aging period up to two years, and found that sands in dry state undergo a time-dependent gain of penetration resistance attributed to mechanical mechanisms, whereas sands in distilled water and sands in sea water undergo a time-dependent gain of penetration resistance attributed to chemical mechanisms. In contrast to the significant time-dependent gain of strength reported later by Schmertmann (1987), Mesri et al. (1990), Schmertmann (1991), Arango and Miguez (1996), and Olson et al. (2001), Baxter (2002) did not observe noticeable increases in mini-cone penetration resistance of sands, after performing lab tests with aging periods ranging from 30 to 118 days. The employment of a small-scale laboratory testing program may be a primary reason that no significant aging effects were observed during this set of experiments.

#### CAPTURING OF SOIL AGING FROM IN-SITU TESTING

Even though the exact mechanisms that cause aging in sands remain unknown, quantitative correlations between in-situ soil indices and aging have been derived for aged soils. For example, Skempton (1986) studied the increase in the SPT blow count with time in five sand deposits and concluded that the aging effect is reflected in higher blow counts and the resistance of sand to deformation is greater the longer the period of consolidation. He found that the increase of the ratio between the normalized SPT blow count,  $(N_1)_{60}$ , and the square of the relative density,  $D_r^2$ , for a normally consolidated 1,000-year-old fine sand would be more than 50% relative to a freshly deposited sand.

Mesri et al. (1990) observed an increase in stiffness of sand due to aging under consolidated or densified conditions. Based on the assumption that cone-penetration resistance is mainly determined by stiffness of sand and effective horizontal stress, they proposed an empirical equation to estimate the increase in cone-penetration resistance with time:

$$\frac{q_c}{(q_c)_R} = \left( \frac{t}{t_R} \right)^{C_D C_a / C_c}, \quad (1)$$

where  $(q_c)_R$  and  $t_R$  are values of cone penetration resistance and time at the end of primary consolidation or some other reference time, and  $q_c$  is cone resistance at any time  $t > t_R$ .  $t_R$  corresponds to the number of days after which postdensification  $q_c$  value was measured and it ranged from 1 to 30 days.  $C_a/C_c$  is the ratio of secondary compression index to compression index, which was found to range between 0.015 and 0.03 for at least nine different sands in the laboratory over a stress range of 50 to 3000 KPa, but as suggested by Mesri et al. (1990), for practical purposes  $C_a/C_c$  for sands can be consid-

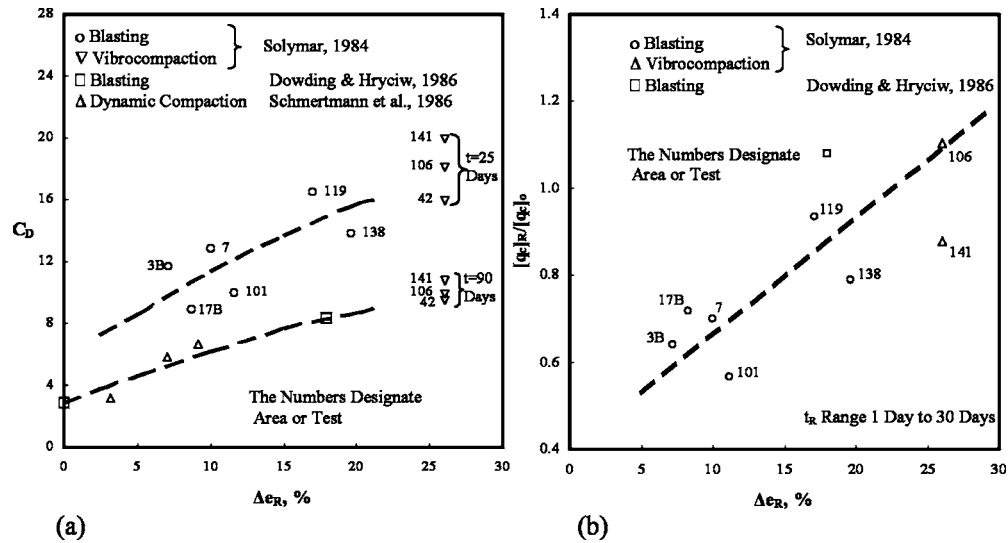


**Figure 1.** Effect of change in relative density due to postliquefaction densification,  $\Delta e_R$ , on (a) the parameter,  $C_D$ , and (b) the ratio of post- to predensification cone penetration resistance (after Mesri et al. 1990).

ered constant and equal to 0.02.  $C_D$  is an empirical parameter introduced to account for the effect of densification due to ground improvement. Blast densification data of Dowding and Hryciw (1986) and deep densification data of Mitchell and Solymar (1984) were used to calibrate Equation 1 by adjusting the parameter,  $C_D$ , until predicted values matched well with the field data. The effect of the change in relative density due to postliquefaction densification,  $\Delta D_r$  or  $\Delta e_R$ , caused by different densification procedures, on the resulting values of  $C_D$ , as well as the ratio  $[q_c]_R/[q_c]_o$  of the post- to the predensification cone penetration resistance is shown in Figure 1.

Kulhawy and Mayne (1990) collected field and laboratory data on SPT blow count  $(N_1)_{60}$  and relative density  $(D_r)$  of both normally consolidated and overconsolidated, unaged sands. They suggested the following empirical relationship for normally consolidated, unaged sands as a function of the soil particle size ( $D_{50}$ ):

$$\frac{(N_1)_{60}}{D_r^2} = 60 + 25 \log D_{50}, \quad (2)$$

Overconsolidated sands and aged sands give higher values than those determined by Equation 2. Based on another set of data representing aged fine to medium sands, likely overconsolidated, of four geologic periods, a correction factor  $c_A$  was introduced by Kulhawy and Mayne (1990) to describe the influence of aging ( $t$ ) on the  $(N_1)_{60}/D_r^2$  ratio:

$$c_A = 1.2 + 0.05 \log(t/100), \quad (3)$$

If the aging coefficient  $c_A$  from Equation 3 is applied on the  $(N_1)_{60}/D_r^2$  ratio for unaged sands from Equation 2, the following relationship is obtained that takes into account the post-earthquake aging process:

$$\frac{(N_1)_{60}}{D_{r(\text{post})}^2} = (60 + 25 \log D_{50}) \cdot (1.2 + 0.05 \log(t/100)) \quad (4)$$

where  $D_{r(\text{post})}$  represents the post-earthquake relative density, which is assumed to remain constant during the entire aging period, and  $(N_1)_{60}$  represents the current SPT penetration resistance of the soil (at time  $t$  after liquefaction or deposition).

### AVAILABLE FIELD DATA

The engineering properties for the source sands at Ten Mile Hill sites A and B, Sampit, and Gapway, as determined by the SPT, CPT, and shear wave velocity data were presented in Hu et al. (2002a) and are summarized in Table 2. The data were obtained in the vicinity of locations where sand blows were or were not found at the four investigated sites in the SCCP. Ten Mile Hill sites A and B involve sand deposits 200,000 years old, whereas older sand deposits 450,000 years old are encountered at the Sampit and Gapway sites.

Paleoliquefaction features at Ten Mile Hill associated with an earthquake that occurred 3,548 years ago (Talwani and Schaeffer 2001) were discovered in a drainage ditch. SPT, CPT, and shear-wave velocity tests were conducted at five locations (TEN-01 to TEN-05) 50 m away from the paleoliquefaction site (Ten Mile Hill site A). SPT tests were not performed at TEN-05. Identical tests were performed at Ten Mile Hill site B (TEN-06 to TEN-10) even though no sand blows were discovered. Both sites were located in an area where widespread liquefaction had been observed in 1886. At the Sampit site, sand blows were found at three locations (SAM-02, SAM-04, and SAM-05) and were associated with earthquake episodes A, B, and C (see Table 1) that occurred 546, 1,021, and 1,648 years ago, respectively. In-situ tests were performed at six locations in total (SAM-01 to SAM-06). At the Gapway site, sand blows were found at three locations (GAP-02, GAP-03, and GAP-04). GAP-02 and GAP-03 were associated with earthquake episodes E and F (see Table 1) that occurred 3,548 and 5,038 years ago, respectively. The sand blow discovered at GAP-04 is assumed to be associated with the same earthquake as the nearby sand blow found at GAP-03.

### CORRECTION OF DATA FOR AGING AND DISTURBANCE

The in-situ geotechnical data collected from the four paleoliquefaction sites are corrected for (1) aging of the soil and (2) disturbance due to postliquefaction consolidation (primary) and densification before they are used in this work to assess the paleoearthquake magnitude and acceleration. By correcting the currently recorded in-situ geotechnical data for aging, the corresponding data immediately after the earthquake (for the sites that liquefied) or deposition (for the sites that did not liquefy) are deter-

**Table 2.** In-situ geotechnical data for source sands (after Hu et al. 2002a)

Site	Location	z (m)	h (m)	$\sigma_o$ (tsf)	$\sigma'_o$ (tsf)	$(N_1)_{60}$	$q_{c1}$ (tsf)	$V_{s1}$ (m/s)	Fines (%)	$D_{50}$ (mm)
Gapway	GAP-01	2	0.7	0.38	0.38	10	33	181	N/A	...
	GAP-02	2	0.9	0.38	0.38	11*	58	220	9	0.15
	GAP-03	2	1.0	0.38	0.38	11	87	177	6	0.19
	GAP-04	2	1.1	0.38	0.38	8	83	240	N/A	...
	GAP-05	2	1.3	0.38	0.38	16	90	154	5	0.20
Sampit	SAM-01	4	5.7	0.74	0.57	14*	114	277	3	0.17
	SAM-02	6	4.3	1.13	0.76	14*	108	250	1	0.16
	SAM-03	5	5.2	0.93	0.67	14*	77	288	0	0.20
	SAM-04	5	5.4	0.93	0.64	14	80	291	2	0.18
	SAM-05	5	5.8	0.93	0.60	16	95	334	4	0.20
	SAM-06	5	5.6	0.93	0.64	9	80	321	4	0.16
Ten Mile Hill A	TEN-01	2	1.5	0.38	0.34	18	163	235	7	0.16
	TEN-02	3	1.5	0.56	0.42	30	204	400	3	0.16
	TEN-03	3	2.4	0.56	0.42	17	159	163	3	0.16
	TEN-04	3	2.7	0.56	0.42	18	83	214	3	0.16
	TEN-05	4	2.4	0.74	0.59	N/A	153	239	N/A	...
Ten Mile Hill B	TEN-06	4	3.8	0.74	0.59	9	46	170	4	0.17
	TEN-07	5	4.1	0.93	0.68	5	57	187	5	0.17
	TEN-08	5	4.2	0.93	0.68	8	57	177	4	0.16
	TEN-09	5	4.3	0.93	0.76	5	60	158	5	0.17
	TEN-10	6	5.3	1.13	0.85	6	66	165	5	0.17

z: depth of the middle point of source sand layer; h: thickness of source sand layer;  $\sigma_o, \sigma'_o$ : total overburden stress and effective overburden stress at the middle point of source sand layer;  $(N_1)_{60}$ : corrected SPT blow count number;  $q_{c1}$ : corrected CPT tip resistance;  $V_{s1}$ : normalized shear-wave velocity; Fines: percentage by weight passing through US #200 sieve;  $D_{50}$ : grain diameter corresponding to 50% passing (by weight) the #200 sieve. \*The blow count values at SAM-01 to SAM-03 are based on data from SAM-04 and at GAP-02 to GAP-05 on the data from GAP-03.

mined. These are termed the “post-earthquake” geotechnical data. The post-earthquake geotechnical data are corrected for disturbance and the corresponding data before the earthquake (for the sites that liquefied) are determined. These are termed “pre-earthquake” geotechnical data. For the sites that did not liquefy, such correction is not required and the “post-earthquake” data are assumed to be equal to the “pre-earthquake” data.

Assuming that the structure and associated aging effects of the source sand have been disrupted at sites where liquefaction occurred due to the earthquake, the soil after the occurrence of liquefaction can be described as “freshly deposited.” Therefore the age of the source sand at the sand-blow locations is equal to the occurrence date of the associated earthquake (see Table 1), assuming that no more liquefaction events have de-

stroyed the soil structure during this period of time. Conversely, at locations where liquefaction did not take place during a prehistoric earthquake and where the soil structure was not disrupted, the age of the source sand is assumed to be equal to the geologic age of the deposit. At Ten Mile Hill site A, the nearest paleoliquefaction feature was approximately 50 m to the northeast. Analysis of the in-situ geotechnical data by Hu et al. (2002a) for all locations (only 23 to 27 m apart from each other) indicated that the soil profile does not significantly change within tens of meters. Therefore it is assumed that the soil properties encountered at TEN-01 to TEN-05 are representative of those 50 m away at the location of the sand blow and the age of the source sand at all five locations is 3,548 years. At Ten Mile Hill site B where no sand blows were discovered, the age of the source sand is equal to 200,000 years. Sand blows at Sampit and Gapway sites were only 10 m and 2m, respectively, away from the borings (Hu et al. 2002a). Thus it is assumed that the properties of the source sand at the vicinity of the sand blows are representative of those at the location of the sand blows. The age of the source sand at SAM-02, SAM-04, SAM-05, GAP-02, GAP-03, and GAP-04 ranges from 546 to 5,038 years, as shown in Table 1. The age of the source sand at the rest of the locations that did not liquefy is 450,000 years.

Since site specific geotechnical data prior to the prehistoric earthquakes is not available, disturbance due to the liquefaction event and postliquefaction aging were estimated using the two approaches currently available in the literature: (1) the Mesri et al. (1990) method and (2) the Kulhawy and Mayne (1990) method.

### APPROACH 1

Mesri et al. (1990) suggested Equation 1 to estimate the increase in CPT penetration resistance following densification resulting from secondary compression only. According to Olson et al. (2001), since both CPT and SPT penetration resistances are affected similarly by soil compressibility and horizontal effective stress, a similar equation can be derived to account for the increase in SPT following densification, by substituting  $N_{60}$  for  $q_c$  in Equation 1. For values of the penetration resistance compared at the same depth,  $N_{60}$  is substituted by  $(N_1)_{60}$ , and  $q_c$  is substituted by  $q_{c1}$ :

$$\frac{q_{c1}}{(q_{c1})_{\text{post}}} = \frac{(N_1)_{60}}{[(N_1)_{60}]_{\text{post}}} = \left(\frac{t}{t_R}\right)^{C_D C_a' C_C}, \quad (5)$$

where  $q_{c1}$  and  $(N_1)_{60}$  are the currently recorded values of CPT and SPT, respectively;  $(q_{c1})_{\text{post}}$  and  $[(N_1)_{60}]_{\text{post}}$  are the post-earthquake values of CPT and SPT, respectively, at time  $t_R$ .  $t_R$  is selected equal to 30 days (=0.082 years). Mesri et al. (1990) accounted for disturbance ( $\Delta e_R$ ) in the ratio of the postdensification to the predensification cone penetration resistance, which was extended by Olson et al. (2001) to the following:

$$\frac{(q_{c1})_{\text{post}}}{(q_{c1})_{\text{pre}}} = \frac{[(N_1)_{60}]_{\text{post}}}{[(N_1)_{60}]_{\text{pre}}}, \quad (6)$$

The correction factor for aging and disturbance that is applied on the  $V_{s1}$  values is

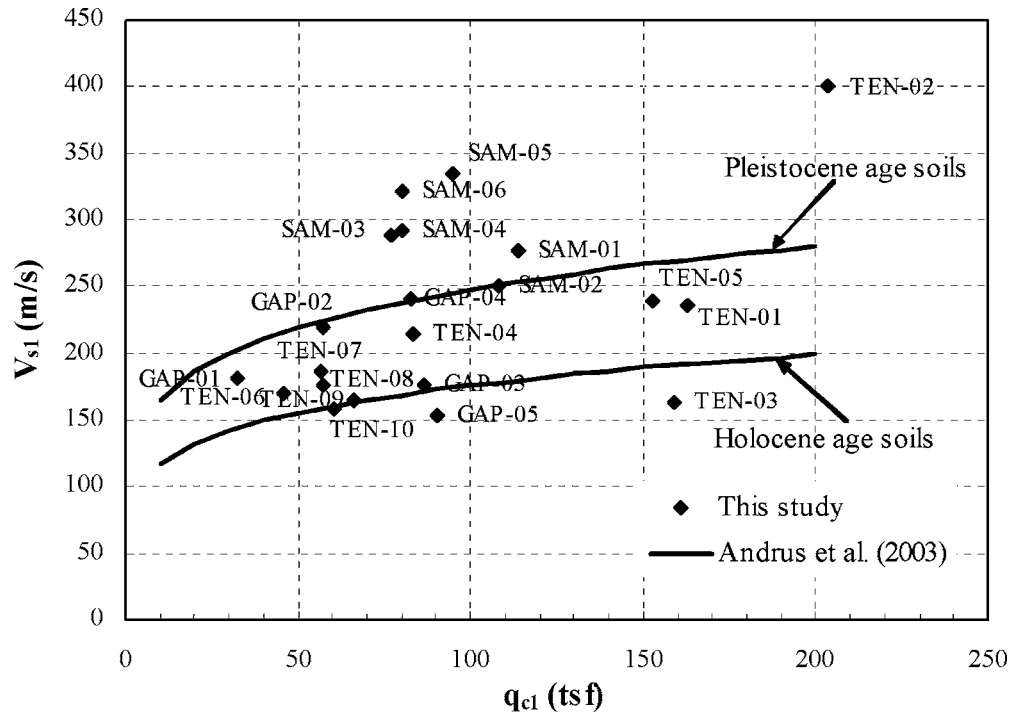


**Figure 2.** Relationship between CPT  $q_{c1}$  values and shear wave velocity  $V_{s1}$  values.

derived by converting the  $V_{s1}$  to equivalent  $q_{c1}$  values where known correction factors are applied. To this end the following correlation proposed by Andrus et al. (2003) is employed:

$$V_{s1} = 77.4(q_{c1})^{0.178} \cdot ASF, \quad (7)$$

where  $V_{s1}$  in m/s,  $q_{c1}$  in tsf, and  $ASF$  is equal to 1.00 for Holocene age deposits (<10,000 years) and equal to 1.41 for Pleistocene age deposits ( $10,000 < t < 1.5$  million years). The above correlation agrees rather well with the data used in this study (CPT versus  $V_s$ ) for all the sites except Sampit (see Figure 2). Solving Equation 7 for  $q_{c1}$  and substituting in Equations 5 and 6 the following relationships are derived for the correction of the currently recorded  $(N_1)_{60}$ ,  $q_{c1}$ , and  $V_{s1}$  values for aging and disturbance:

$$\frac{(N_1)_{60}}{[(N_1)_{60}]_{\text{post}}} = \frac{q_{c1}}{(q_{c1})_{\text{post}}} = \left[ \frac{(V_{s1})}{(V_{s1})_{\text{post}}} \right]^{1/0.178} = \left( \frac{t}{t_R} \right)^{C_D C_d' C_C}, \quad (8)$$

$$\frac{[(N_1)_{60}]_{\text{post}}}{[(N_1)_{60}]_{\text{pre}}} = \frac{(q_{c1})_{\text{post}}}{(q_{c1})_{\text{pre}}} = \left[ \frac{(V_{s1})_{\text{post}}}{(V_{s1})_{\text{pre}}} \right]^{1/0.178}, \quad (9)$$

The value of  $\Delta e_R$ , was estimated by Ellis and de Alba (1999) to be around 4 to 5%; and Stark et al. (2002) suggested 4 to 10%. Therefore two values of  $\Delta e_R$ , 5% and 10%, are selected in this study to represent the possible range of change in relative density due to postliquefaction densification. So from Figure 1 and  $\Delta e_R$  equal to 5%,  $C_D$  is found equal to 5.5 (Figure 1a) and Equation 9 becomes equal to 0.55 (Figure 1b). Similarly for  $\Delta e_R$  equal to 10%,  $C_D$  is equal to 7.0 and Equation 9 becomes equal to 0.67. It should be noted that for locations that did not liquefy and, as such, a disturbance mechanism (as expressed by  $C_D$ ) never existed, the Mesri et al. (1990) method cannot be used.

## APPROACH 2

Kulhawy and Mayne (1990) proposed a correction factor  $c_A$  as described by Equation 3 to introduce the effect of aging on the  $(N_1)_{60}/D_r^2$  ratio. According to Kulhawy (2003), the same coefficient can be applied to CPT penetration resistance data. Similar to Approach 1, the correction factor that is applied on the shear-wave velocity data is derived by converting the  $V_{s1}$  to equivalent  $q_{c1}$  values using Equation 7. Thus the correction for aging of the currently recorded  $(N_1)_{60}$ ,  $q_{c1}$ , and  $V_{s1}$  data with the Kulhawy and Mayne (1990) method can be described by the following equation:

$$\frac{(N_1)_{60}}{[(N_1)_{60}]_{\text{post}}} = \frac{q_{c1}}{(q_{c1})_{\text{post}}} = \left[ \frac{(V_{s1})}{(V_{s1})_{\text{post}}} \right]^{1/0.178} = c_A, \quad (10)$$

According to Ellis and de Alba (1999), after liquefaction and dissipation of seismically induced pore water pressure, the relative density of the soil increases, therefore

$$D_{r(\text{pre})} = D_{r(\text{post})} - \Delta D_r \quad (11)$$

$$(N_1)_{60(\text{pre})} = (N_1)_{60(\text{post})} - [\Delta(N_1)_{60}] \quad (12)$$

where  $D_{r(\text{pre})}$  and  $(N_1)_{60(\text{pre})}$  are the pre-earthquake relative density and SPT blow count, respectively;  $D_{r(\text{post})}$  and  $(N_1)_{60(\text{post})}$  are the post-earthquake relative density and SPT blow count, respectively; and  $\Delta D_r$  and  $\Delta(N_1)_{60}$  are the change in relative density and SPT blow count, respectively, due to postliquefaction consolidation (disturbance effect). By differentiating Equation 2 with respect to  $D_r$ , the following relationship is obtained:

$$\Delta(N_1)_{60} = 2 \cdot D_{r(\text{pre})} \cdot \Delta D_r \cdot (60 + 25 \log D_{50}) \quad (13)$$

Once  $D_{r(\text{post})}$  has been calculated from Equation 4, Equation 11 is used to calculate the  $D_{r(\text{pre})}$  for two different values of the change in relative density:  $\Delta D_r = 5\%$  and  $10\%$ .  $\Delta(N_1)_{60}$  is then calculated from Equation 13 and substituted in Equation 12 to determine  $(N_1)_{60(\text{pre})}$ .

To estimate the change in CPT penetration resistance due to postliquefaction consolidation  $\Delta(q_{c1})$ , the CPT data are converted to equivalent SPT data and Equation 13 is employed again. To this end, correlations between SPT and CPT are developed specifically for each one of the four sites, as shown in Figure 3. A linear approximation can be made from the data for each of the four sites such that the change in CPT value will be directly proportional to the change in SPT value:

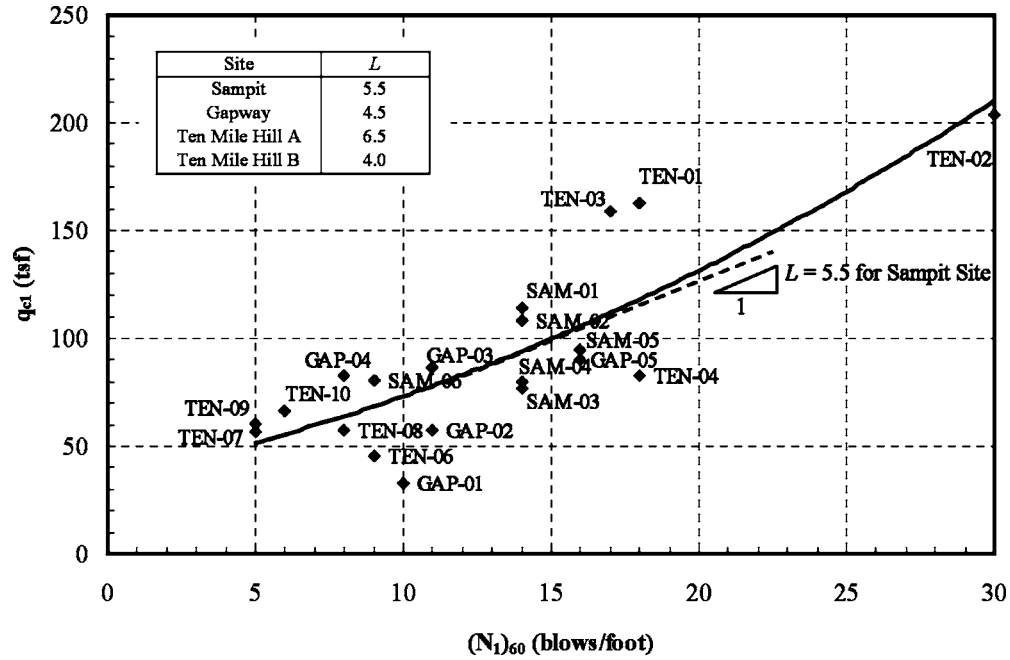


**Figure 3.** Currently recorded SPT data  $(N_1)_{60}$  versus the currently recorded CPT data  $(q_{c1})$  at the four investigated sites.

$$\Delta(q_{c1}) \cong L \cdot \Delta(N_1)_{60} \quad (14)$$

where the values of  $L$  and the valid range of  $q_{c1}$  are shown in Figure 3 for the four sites.

In this case, the post-earthquake relative density  $D_{r(\text{post})}$  is determined using the equation

$$\frac{q_{c1}}{D_r^2} = 305 \quad (15)$$

proposed by Kulhawy and Mayne (1990) for unaged sands, where the aging coefficient  $c_A$  from Equation 3 is applied to take into account the post-earthquake aging process:

$$\frac{q_{c1}}{D_{r(\text{post})}^2} = 305 \cdot (1.2 + 0.05 \log(t/100)) \quad (16)$$

where  $q_{c1}$  (in tsf) represents the currently recorded CPT penetration resistance of the soil (at time  $t$  after liquefaction or deposition). Once the equivalent  $\Delta(N_1)_{60}$  values are calculated with the process just described they are converted into  $\Delta(q_{c1})$  values using Equation 14 and data in Table 3. Similarly to the SPT, the pre-earthquake CPT penetration resistance  $(q_{c1})_{(\text{pre})}$  is determined as

**Table 3.** Penetration resistance and shear wave velocity data for source sands corrected for aging and disturbance

			Pre-Earthquake In-situ Geotechnical Data for Source Sands											
			Approach 1 (Mesri et al. 1990)						Approach 2 (Kulhawy and Mayne 1990)					
			$\Delta D_r=5\%$			$\Delta D_r=10\%$			$\Delta D_r=5\%$			$\Delta D_r=10\%$		
Site	Location	$t(\text{years})$	$(N_1)_{60}$	$q_{c1}$ (tsf)	$V_{s1}$ (m/s)	$(N_1)_{60}$	$q_{c1}$ (tsf)	$V_{s1}$ (m/s)	$(N_1)_{60}$	$q_{c1}$ (tsf)	$V_{s1}$ (m/s)	$(N_1)_{60}$	$q_{c1}$ (tsf)	$V_{s1}$ (m/s)
Gapway	GAP-01	450,000	--	--	--	--	--	--	7	24	171	7	24	171
	GAP-02	3,548	6	32	199	4	19	181	7	39	210	6	35	209
	GAP-03	5,038	6	47	159	4	28	144	7	59	166	6	53	164
	GAP-04	5,038*	4	45	215	3	27	196	5	57	159	4	51	156
	GAP-05	450,000	--	--	--	--	--	--	12	65	145	12	65	145
Sampit	SAM-01	450,000	--	--	--	--	--	--	10	82	261	10	82	261
	SAM-02	546	10	75	234	6	47	216	9	77	240	8	68	239
	SAM-03	450,000	--	--	--	--	--	--	10	56	272	10	56	272
	SAM-04	1,021	9	52	269	6	32	247	9	55	279	8	48	279
	SAM-05	1,648	10	58	306	6	35	280	11	65	320	9	56	320
	SAM-06	450,000	--	--	--	--	--	--	7	58	303	7	58	303
Ten Mile Hill A	TEN-01	3,548	10	91	212	6	55	193	12	112	223	10	99	222
	TEN-02	3,548	17	115	361	10	68	329	21	142	383	18	127	383
	TEN-03	3,548	10	90	147	6	53	134	11	109	146	9	97	136
	TEN-04	3,548	10	47	193	6	28	176	12	54	203	10	46	202
	TEN-05	3,548	--	86	216	--	51	197	--	104	227	--	92	226
Ten Mile Hill B	TEN-06	200,000	--	--	--	--	--	--	7	33	161	7	33	161
	TEN-07	200,000	--	--	--	--	--	--	4	42	177	4	42	177
	TEN-08	200,000	--	--	--	--	--	--	6	42	167	6	42	167
	TEN-09	200,000	--	--	--	--	--	--	4	44	149	4	44	149
	TEN-10	200,000	--	--	--	--	--	--	4	48	156	4	48	156

\*The sand blow at GAP-04 was not associated with a prehistoric earthquake, so its age is based on the age of the adjacent sand blow at GAP-03.

$$(q_{c1})_{pre} = (q_{c1})_{post} - \Delta(q_{c1}) \quad (17)$$

For the shear-wave velocity data, the correlation by Andrus et al. (2003) is employed (Equation 7) to convert the post-earthquake  $(V_{s1})_{post}$  to equivalent  $(q_{c1})_{post}$  values. The same steps as for the calculation of the  $(q_{c1})_{pre}$  values are followed. Once the equivalent  $(q_{c1})_{pre}$  are calculated, Equation 7 is used again to convert to  $(V_{s1})_{pre}$  values.

The pre-earthquake SPT, CPT, and  $V_s$  values at each location are presented in Table 3 based on the described Approach 1 and Approach 2. It is noted that for the same disturbance due to liquefaction ( $\Delta D_r$  value), the estimated pre-earthquake SPT and CPT values with the two different approaches are in a good agreement. The higher the disturbance, the higher the difference observed between the results with the two approaches, but on the average they differ by approximately 10% for  $\Delta D_r$  equal to 5% and by approximately 20% for  $\Delta D_r$  equal to 10%. For example, the current  $(N_1)_{60}$  value of 16 for SAM-05 decreases to the pre-earthquake value of 10 and 11 for Approach 1 and 2, respectively, when  $\Delta D_r=5\%$ , and to a value of 6 and 9 when  $\Delta D_r=10\%$ . Similarly, the current  $q_{c1}$  value of 95 tsf for the same site decreases to the pre-earthquake value of 58 tsf and 65 tsf for Approach 1 and 2, respectively, when  $\Delta D_r=5\%$ , and to a value of 35 tsf and 56 tsf when  $\Delta D_r=10\%$ . In general, very small changes are noted in the shear-wave velocity values when the correction for aging and disturbance is applied. In particular, the currently recorded shear wave values differ from the pre-earthquake calculated values by approximately 7%.

## PALEOEARTHQUAKE ASSESSMENT METHODS

### PALEOEARTHQUAKE MAGNITUDE ASSESSMENT

In a paleoliquefaction study, magnitudes of prehistoric earthquakes can be estimated from the regional distribution of their associated liquefaction features. Accordingly, the method of inferring earthquake magnitude from paleoliquefaction studies involves associating each paleoliquefaction evidence with a prehistoric earthquake (as in Table 1) and back-calculating the magnitude of the earthquake using available techniques. In this study, the Magnitude-Bound (Ambraseys 1988) and the Energy-Stress (Pond and Martin 1997) methods are used.

The Magnitude-Bound method estimates the magnitude of a paleoearthquake by using relations between earthquake magnitude and distance from the tectonic source to the farthest site of liquefaction. This method is based on field observations that demonstrate an upper bound of the epicentral distance  $R_e$ , beyond which liquefaction is not usually observed during an earthquake of magnitude  $M$ . Back-calculation of the earthquake magnitude using the Energy-Stress method is based on a relationship between the seismic intensity at the site in terms of magnitude  $M$  and hypocentral distance  $R$  with the liquefaction susceptibility as represented by the  $(N_1)_{60}$  blow count of the soil. Hu et al. (2002b) derived a relationship based on Pond and Martin's (1997) work that can be used to predict the magnitude  $M$  of the earthquake required to induce liquefaction at a site of known hypocentral distance  $R$  with a certain value of  $(N_1)_{60}$ . Details and limitations of these two methods are discussed elsewhere (Hu et al. 2002b, Obermeier and Pond 1999, Obermeier et al. 2001).

## PALEOEARTHQUAKE ACCELERATION ASSESSMENT

Most of the methods available for evaluating the acceleration at a specific site are based on correlations between some in-situ characteristics of the potentially liquefiable soil that represent the resisting strength of the soil to liquefaction and the magnitude of the earthquake. In this study, the Seed et al. (1985) Cyclic Stress method, the Ishihara (1985) method, and the Martin and Clough (1994) method are used. A brief summary of each method is presented herein. Limitations associated with using the methods for back-analysis are discussed in detail elsewhere (Hu et al. 2002b, Obermeier and Pond 1999, Obermeier et al. 2001, Olson et al. 2001).

The Seed et al. (1985) Cyclic Stress method relates earthquake shaking to surficial liquefaction evidence and is a few steps forward of the originally proposed “simplified” method of Seed and Idriss (1971). The approach is based on field observations of the performance of sand deposits that did or did not liquefy in previous earthquakes worldwide. The earthquake-induced (horizontal) cyclic shear stress is compared to the cyclic resistance of the soil. The cyclic shear stress is a function of the earthquake magnitude, peak surface acceleration, the total and effective overburden stress, and the depth of the source bed. The cyclic resistance has been correlated with in-situ “index” tests such as the SPT blow count and the CPT tip resistance (Youd et al. 2001) and the shear wave velocity (Andrus and Stokoe 2000) of the soil.

The Ishihara (1985) method is based upon the hypothesis that the maximum height of dikes, accompanied by venting at the surface, is controlled by the thickness of the liquefied sediment and the peak acceleration. Ishihara (1985) investigated the conditions where evidence of liquefaction in deeper layers is suppressed by a resistant, or protective, surface layer. He developed an empirical correlation, which provides approximate peak acceleration boundaries for liquefaction-induced surface damage for soil profiles consisting of a liquefiable layer overlain by the nonliquefied cap layer. Youd and Garris (1995) found that the thickness bounds proposed by Ishihara (1985) appear valid only for the prediction of ground surface disruptions at sites that were not susceptible to ground oscillation or lateral spread.

The Martin and Clough (1994) method is based upon the idea that the threshold acceleration level must lie between those estimated by Seed’s simplified procedure and those estimated by Ishihara’s guideline. Seed’s Cyclic Stress method was developed from field observations at the surface after the earthquakes and does not consider the influence of cap thickness on liquefaction-induced ground failure, which can have a significant effect on whether dikes have penetrated partially or completely. Ishihara, on the other hand, produced estimates of the thickness of the cap layer required to prevent level-ground liquefaction-related damage. Seed’s method can be used to determine which layers within the soil profile would liquefy under various levels of peak acceleration. For each one of the acceleration levels Ishihara curves can determine whether the liquefied layers were sufficiently thick to allow sand blows to be formed at the ground surface. The lowest value of peak ground acceleration at which both methods agree that sand blows would be formed is considered the threshold acceleration.

**Table 4.** Paleoearthquake magnitude assessment using the Energy-Stress and the Magnitude-Bound methods

Episode	Associated Sand Blow	Energy-Stress Method						Magnitude-Bound Method
		Average $(N_1)_{60(\text{pre})}$ for Source Sands		This Study		Hu et al. (2002b)		
		$\Delta D_r=5\%$	$\Delta D_r=10\%$	$\Delta D_r=5\%$	$\Delta D_r=10\%$			
A	SAM-02	10	7	6.8 to 7.0	6.2 to 6.4	7.4 to 7.6	6.9 to 7.1	
B	SAM-04	9	7	6.6 to 6.8	6.2 to 6.4	7.4 to 7.6	6.9 to 7.1	
C	SAM-05	11	8	5.6 to 6.4	5.1 to 5.8	6.3 to 7.0	5.7 to 6.3	
C'	SAM-05	11	8	7.0 to 7.2	6.4 to 6.6	7.6 to 7.8	6.9 to 7.1	
E	GAP-02	7	5	6.2 to 6.4	5.6 to 5.8	6.8 to 7.0	6.9 to 7.1	
F	GAP-03	7	5	4.9 to 5.6	4.3 to 5.0	5.5 to 6.2	5.7 to 6.3	
F'	GAP-03	7	5	5.9 to 6.1	5.6 to 5.8	6.8 to 7.0	6.9 to 7.1	
?	TMHA	11	8	5.6 to 6.4	5.1 to 5.8	6.5 to 7.2	5.7 to 6.3	

## RESULTS

The first step was to estimate the magnitudes of the seven prehistoric earthquakes from the regional distribution of their associated liquefaction features and the geotechnical engineering data that characterize these sites. The results for the Energy-Stress and the Magnitude-Bound methods are presented in Table 4. For the application of the Magnitude-Bound method it is assumed that the sand blow associated with a specific earthquake is the furthest liquefaction feature (epicentral distance  $R_e$  in Table 4) that was caused by this event. For the application of the Energy-Stress method, the SPT blow counts  $(N_1)_{60(\text{pre})}$  that have been corrected for aging and disturbance are used. It is believed that these values more realistically represent the strength of the soil at the time of the earthquake.  $(N_1)_{60(\text{pre})}$  were calculated using two different approaches (Approaches 1 and 2) and two different values (5 and 10%) of the change in relative density ( $\Delta D_r$  or  $\Delta e_R$ ) due to postliquefaction consolidation. For the same disturbance due to liquefaction ( $\Delta D_r=5\%$  or  $10\%$ ), the estimated  $(N_1)_{60(\text{pre})}$  values with the two different approaches are in a good agreement (see Table 3). Therefore the average of the two approaches for each  $\Delta D_r$  pre-earthquake  $(N_1)_{60}$  is used for the magnitude assessment. The distance from the source is assumed to be the hypocentral distance (R in Table 4), which is reasonable since the depth to the Charleston source is known to be  $10 \pm 3$  km. For the range of the hypocentral distances from the earthquake source, a range of magnitudes is calculated.

It is noted that the higher the disturbance due to the liquefaction event ( $\Delta D_r$ ), the lower the estimated earthquake magnitude. On average the estimated magnitudes with  $\Delta D_r=5\%$  and  $\Delta D_r=10\%$  do not differ by more than 0.5 units. The earthquake magnitudes estimated in this study are lower than the results by Hu et al. (2002b). By using the current  $(N_1)_{60}$  values to represent the soil resistance at the time of the earthquake, Hu et al. (2002b) provided more conservative (higher) estimates of the prehistoric earthquake

magnitudes. The estimated magnitudes from this study differ from the ones by Hu et al. (2002b) by approximately 0.7 units when  $\Delta D_r=5\%$ , and 1.2 units when  $\Delta D_r=10\%$ .

Even though Ten Mile Hill was not in the immediate vicinity of any dated sand blows, the associated seismic source for the liquefaction at Ten Mile Hill site A was assumed to be near the Charleston source with a hypocentral distance of 10 to 35 km. The representative pre-earthquake  $(N_1)_{60}$  value of 10 from Ten Mile Hill site A was used to back-calculate the threshold earthquake magnitude for extensive liquefaction at Ten Mile Hill A.

Some of the estimated earthquake magnitudes with the Energy-Stress method are inconsistent with previous observations (Obermeier 2001), which indicate M5.5 as the lowest earthquake magnitude capable of producing liquefaction. This is observed especially for the inferred change in relative density  $\Delta D_r=10\%$ , indicating that it is probably very high and it did not actually take place. In addition, the Energy-Stress method is sensitive to the SPT blow count and results in significant changes in M for small changes in  $(N_1)_{60}$ . Unfortunately, the number of corrections (Skempton 1986; Kulhawy and Mayne 1990; Robertson and Wride 1997, 1998) that must be made to the raw SPT data from even the most carefully conducted tests leads to a large amount of uncertainties incorporated in a reported N value.

The second step was to use the Cyclic-Stress method, the Ishihara method, and the Martin and Clough method to estimate the threshold peak ground acceleration corresponding to earthquake magnitudes M6 and M7.5 at the four sites. These magnitudes were considered representative of earthquake magnitudes in the SCCP and were used instead of the site specific magnitudes determined in the first step to illustrate how the peak ground accelerations would vary from site to site for the same earthquake magnitude.

Because locations were found in the same site that had both liquefied and not liquefied during the prehistoric earthquakes, they pose a lower and an upper bound, respectively, of the estimated acceleration in an area. At the locations where the soil liquefied, the resistance of the soils was exceeded, and therefore these sites provide a lower bound. At the locations where the soil did not liquefy, the resistance was not reached, and therefore these locations provide an upper bound of the threshold acceleration. However, all the locations are taken into account for the estimation of the threshold acceleration in the site they are located, assuming that the factor of safety at the time of the earthquake was equal to one (marginal liquefaction).

With the Cyclic Stress method, the resistance of the soil as expressed by the in-situ soil indices (SPT, CPT,  $V_s$ ) is taken into consideration, assuming a freshly deposited soil prior to the earthquake at the sites where liquefaction occurred. Since field observations of sites with aged soils might also have been incorporated by Seed et al. (1985), an aged soil deposit can be assumed prior to the earthquake at the paleoliquefaction sites and still yield reliable threshold peak ground acceleration results using the aforementioned method. Similar to the Energy-Stress method, the average of the two approaches  $(N_1)_{60(\text{pre})}$ ,  $q_{c1(\text{pre})}$ , and  $V_{s1(\text{pre})}$  are used at each location since the estimated values with the two different approaches are in a good agreement for the same disturbance due to

**Table 5.** Threshold peak ground accelerations back-calculated from the Cyclic Stress method for each site

Threshold Peak Ground Acceleration		SPT-based			CPT-based			$V_s$ -based		
Earthquake Magnitude	Site	This Study		Hu et al. (2002b)	This Study		Hu et al. (2002b)	This Study		Hu et al. (2002b)
		$\Delta D_r=5\%$	$\Delta D_r=10\%$		$\Delta D_r=5\%$	$\Delta D_r=10\%$		$\Delta D_r=5\%$	$\Delta D_r=10\%$	
M=7.5	Gapway	0.11–0.20	0.10–0.20	0.14–0.27	0.11–0.17	0.10–0.17	0.13–0.23	0.11–0.18	0.11–0.18	0.13–0.22
	Sampit	0.06–0.10	0.08–0.13	0.11–0.20	0.10–0.16	0.08–0.16	0.14–0.28	0.09–0.12	0.09–0.12	N/A
	TMHA	0.11–0.20	0.09–0.17	0.21–0.59	0.11–0.33	0.09–0.22	0.15–0.54	0.09–0.37	0.07–0.34	0.11
	TMHB	0.07–0.10	0.07–0.10	0.08–0.12	0.10–0.11	0.10–0.11	0.11–0.13	0.10–0.15	0.10–0.15	0.12–0.20
M=6.0	Gapway	0.22–0.39	0.19–0.39	0.24–0.48	0.21–0.32	0.19–0.32	0.23–0.41	0.22–0.35	0.22–0.35	0.23–0.39
	Sampit	0.17–0.26	0.16–0.26	0.19–0.35	0.19–0.31	0.16–0.31	0.25–0.50	0.18–0.23	0.18–0.23	N/A
	TMHA	0.25–0.45	0.18–0.32	0.37–1.03	0.21–0.64	0.18–0.42	0.27–0.95	0.17	0.14	0.20
	TMHB	0.13–0.19	0.13–0.19	0.14–0.22	0.19–0.22	0.19–0.22	0.19–0.23	0.20–0.29	0.20–0.29	0.20–0.28

**Table 6.** Threshold peak ground accelerations back-calculated from the Martin and Clough (1994) method for each site

Earthquake Magnitude	Site	Threshold Peak Ground Acceleration		
		This Study		Hu et al. (2002b)
		$\Delta D_r=5\%$	$\Delta D_r=10\%$	
M=7.5	Gapway	0.12	0.11	0.19
	Sampit	0.12	N/A	0.19
	TMHA	0.24	0.24	0.37
	TMHB	N/A	N/A	0.20
M=6.0	Gapway	0.16	0.15	0.25
	Sampit	0.15	0.12	0.25
	TMHA	0.30	0.25	0.46
	TMHB	0.18	0.18	0.23

liquefaction ( $\Delta D_r=5\%$  or  $10\%$ ) (see Table 3). For the SPT- and CPT-based procedure, the Youd et al. (2001) empirical correlations are employed, whereas for the  $V_s$ -based procedure, the Andrus and Stokoe (2000) empirical correlation is employed for earthquake magnitude M7.5. The estimated accelerations for earthquake magnitude M7.5 and M6.0 for the SPT-, CPT-, and  $V_s$ -based procedure are presented in Table 5. The value of the magnitude scaling factor (MSF) used is the average value from the range recommended by Youd and Idriss (1997). The estimated accelerations differ from the ones by Hu et al. (2002b), depending on the procedure used. On average, the difference in results is approximately 30%, for the SPT-based procedure, 25% for the CPT-based procedure, and 20% for the  $V_s$ -based procedure. If the lower bound value of the MSF is used per the recommendation of Idriss and Boulanger (2004) and Seed et al. (2001), then the back-calculated peak ground accelerations reported in this study would be 0.005 g to 0.03 g less.

The peak ground accelerations using the Ishihara (1985) method are the same for this study as presented by Hu et al. (2002b) because soil properties are not used in the analysis. The method gives only a rough estimate of the minimum peak ground acceleration that can cause sand blows at a specific site in part because the soil properties such as relative density and fines content are not considered in the analysis. Therefore the Martin and Clough method, which combines the Ishihara method with the Cyclic Stress method, was used to provide a more reliable estimate of the back-calculated threshold peak ground accelerations. The results are summarized in Table 6. The estimated threshold accelerations from this study are lower than the ones obtained by Hu et al. (2002b) for reasons similar to those explained when using the Cyclic Stress method. The difference is on the order of 35%, and for  $\Delta_r=5\%$  and 40% for  $\Delta_r=10\%$ .

The threshold peak ground accelerations independent of  $\Delta D_r$  are summarized for all methods in Table 7. For the Cyclic Stress method, since the results for  $\Delta D_r=5\%$  and

**Table 7.** Estimated peak ground accelerations for each site

Earthquake Magnitude	Site	Estimated Peak Ground Accelerations (g)				
		Ishihara Method	Cyclic Stress Method			Martin & Clough Method
			SPT	CPT	$V_s$	
M=7.5	Gapway	0.20	0.10 to 0.20	0.10 to 0.17	0.11 to 0.18	0.12
	Sampit	0.20	0.06 to 0.13	0.08 to 0.16	0.09 to 0.12	0.12
	TMHA	0.30	0.09 to 0.20	0.09 to 0.33	0.07 to 0.37	0.24
	TMHB	0.20	0.07 to 0.10	0.10 to 0.11	0.10 to 0.15	N/A
M=6.0	Gapway	—	0.19 to 0.39	0.19 to 0.32	0.22 to 0.35	0.16
	Sampit	—	0.16 to 0.26	0.16 to 0.31	0.18 to 0.23	0.14
	TMHA	—	0.18 to 0.45	0.18 to 0.64	0.14 to 0.17	0.28
	TMHB	—	0.13 to 0.19	0.19 to 0.22	0.20 to 0.29	0.18

10% differ up to 25% and overlap considerably (Table 5), the envelope of accelerations is preferred. For the Martin and Clough method the results for  $\Delta D_r=5\%$  and 10% (Table 7) differ only slightly, so the average is preferred.

Finally, the site-specific estimated magnitudes for the prehistoric earthquakes determined from the Energy-Stress method and the pre-earthquake SPT blow counts ( $N_1$ )<sub>60</sub> (average of Approach 1 and 2, see Table 3) at the location of sand blows were used to back-calculate the minimum peak ground accelerations that could cause sand blows for these prehistoric earthquakes using the Cyclic-Stress method. These peak ground accelerations and magnitudes for the seven prehistoric episodes are presented in Table 8 and

**Table 8.** Estimated magnitudes and peak ground accelerations of prehistoric earthquake episodes in SCCP

Episode	Estimated Magnitudes			Estimated Peak Ground Accelerations (g)		
	Talwani & Schaeffer (2001)		Hu et al. (2002b)	This Study	Hu et al. (2002b)	This Study
	Empirical	Magnitude Bound				
A	7+	7.0	7.4 to 7.6	6.2 to 7.0	0.16 to 0.18	0.14
B	7+	7.0	7.4 to 7.6	6.2 to 6.8	0.16 to 0.18	0.14 to 0.15
C	~6	6.3 to 6.8	6.3 to 7.0	5.1 to 6.4	0.21 to 0.28	0.20 to 0.29
C'	7+	7.2	7.6 to 7.8	6.4 to 7.2	0.16 to 0.17	0.14 to 0.15
D	~6	5.7			0.23 to 0.24	0.21 to 0.26
E	7+	7.0	6.8 to 7.0	5.6 to 6.4	0.31 to 0.42	0.30 to 0.53
F	~6		5.5 to 6.2	4.3 to 5.6	0.23 to 0.24	0.22 to 0.24
F'	7+		6.8 to 7.0	5.5 to 6.2		
G	7+	7.2				

are compared with the magnitudes and peak ground accelerations derived from previous studies by Talwani and Schaeffer (2001) and Hu et al. (2002b). In general, the estimated magnitudes from this study are lower than the ones by Hu et al. (2002b) by approximately 0.9 units. Peak ground accelerations determined by Hu et al. (2002b) on the order of 0.15 g are estimated to be 15% lower in this study for the same episodes. However, for episodes with higher peak ground acceleration values determined by Hu et al. (2002b), ( $>0.20$  g) gave almost identical values with the ones determined in this study.

### SUMMARY AND CONCLUSIONS

This work employed available methods for the evaluation of the prehistoric earthquake magnitudes and peak ground acceleration from the spatial distribution of paleoliquefaction features and in-situ geotechnical data. The magnitude of the prehistoric earthquakes was estimated by the Magnitude-Bound (Ambraseys 1988) and the Energy-Stress (Pond and Martin 1997) methods, whereas the peak ground acceleration was estimated by Seed's (1985) Cyclic Stress method, the Ishihara (1985) method, and the Martin and Clough (1994) method. For those methods that account for the resistance of the source sand as expressed by the in-situ geotechnical data (SPT, CPT,  $V_s$ ), these data were corrected for the effect of aging and disturbance due to liquefaction using correlations proposed by Mesri et al. (1990) and Kulhawy and Mayne (1990). Hence the penetration resistance or shear wave velocity before the earthquake was employed to more realistically represent the strength of the soil at that time. The findings of this study are as follows:

- Accounting for aging of the old sand deposits in the SCCP lowered the estimated prehistoric earthquake magnitudes by about 0.9 units.
- For the same episodes, accounting for aging lowered the estimated peak ground accelerations by 15% for those events originally estimated at  $\sim 0.15$  g. For events originally estimated at  $>0.2$  g, there were no changes when aging corrections were applied.
- For a given earthquake magnitude, the estimated minimum peak ground accelerations induced by the SCCP prehistoric earthquakes were approximately 25% lower when aging corrections were applied than when they were not.
- The prehistoric earthquakes that occurred during the past 6,000 years and caused paleoliquefaction features in the SCCP are estimated to have magnitudes between about 5 and 7 and peak ground accelerations between about 0.15 and 0.30 g when aging effects are considered.

### ACKNOWLEDGMENTS

The writers wish to thank Bechtel Savannah River Company for providing the CPT and shear-wave velocity data. The SPT were collected with funding provided by the Nuclear Regulatory Commission. Deep appreciation is extended to Mike Lewis from Westinghouse Savannah River Company for his helpful comments and valuable suggestions. Finally, the first author is indebted to her employer Panagiotis Vettas of OTM, Inc., Greece, for his support during the course of this study.

## REFERENCES

- Ambraseys, N. N., 1988. Engineering seismology, *Earthquake Eng. Struct. Dyn.* **17**, 1–105.
- Andrus, R. D., Piratheepan, P., and Juang, C. H., 2003. Shear wave velocity—Penetration resistance correlations for ground shaking and liquefaction hazards assessment; <http://erpweb.er.usgs.gov/reports/annsum/vol43/pt/01g0007.pdf> (2/08/03)
- Andrus, R. D., and Stokoe, K. H., II, 2000. Liquefaction resistance of soils from shear wave velocity, *J. Geotech. Geoenviron. Eng.* **126** (11), 1015–1025.
- Arango I., and Miguez, R. E., 1996. Investigation of the seismic liquefaction of old sand deposits, *Report on Research, Bechtel Corporation, National Science Foundation Grant No. CMS-94-16169*, San Francisco, CA.
- Baxter, C. D. P., 2002. An Experimental Study on the Aging of Sands, dissertation submitted to the Faculty of the Virginia Polytechnic Institute and State University, Blacksburg, VA.
- Dowding, C. H., and Hryciw, R. D., 1986. A laboratory study of blast densification of saturated sand, *J. Geotech. Eng.* **112** (2), 187–199.
- Ellis, C., and De Alba, P., 1999. Acceleration distribution and epicentral location of the 1755 Cape Ann earthquake from case histories of ground failure, *Seismol. Res. Lett.* **70** (6), 758–773.
- Hu, K., Gassman, S. L., and Talwani, P., 2002a. In-situ properties of soils at paleoliquefaction sites in the South Carolina Coastal Plain, *Seismol. Res. Lett.* **73** (6), 964–978.
- Hu, K., Gassman, S. L., and Talwani, P., 2002b. Magnitudes of prehistoric earthquakes in the South Carolina Coastal Plain from geotechnical data, *Seismol. Res. Lett.* **73** (6), 979–991.
- Idriss, I. M., and Boulanger, R. W., 2004. Semi-empirical procedures for evaluating liquefaction potential during earthquakes, *Proceedings of 11th International Conference on Soil Dynamics and Earthquake Engineering and the 3rd International Conference on Earthquake Geotechnical Engineering, Berkeley, CA.*
- Ishihara, K., 1985. Stability of natural soils during earthquakes, *Proceedings of 11th International Conference on Soil Mechanics and Foundation Engineering, San Francisco, A.A. Balkema, Rotterdam/Boston*, vol. 1, pp. 321–376.
- Joshi R. C., Achari, G., Kaniraj, S. R., and Wijeweera, H., 1995. Effect of aging on the penetration resistance of sands, *Can. Geotech. J.* **32** (5), 767–782.
- Kulhawy, F. H., and Mayne, P. W., 1990. Manual on Estimating Soil Properties for Foundation Design, Final Report 1493-6, EL-6800, Electric Power Research Institute, Palo Alto, CA.
- Martin, J. R., and Clough, G. W., 1994. Seismic parameters from liquefaction evidence, *J. Geotech. Eng.* **120** (8), 1345–1361.
- Mesri, G., Feng, T. W., and Benak, J. M., 1990. Postdensification penetration resistance of clean sands, *J. Geotech. Eng.* **116** (7), 1095–1115.
- Mitchell, J. K., 1986. Practical problems from surprising soil behavior, The 20th Terzaghi Lecture, *J. Geotech. Eng.* **112** (3), 259–289.
- Mitchell, J. K., and Solymar, Z. V., 1984. Time dependent strength gain in freshly deposited or densified sand, *J. Geotech. Eng.* **110** (11), 1559–1576.
- Obermeier, S. F., and Pond, E. C., 1999. Issues in using liquefaction features for paleoseismic analysis, *Seismol. Res. Lett.* **70** (1), 34–58.
- Obermeier, S. F., Olson, S. M., Pond, E., Green, R., Stark, T. D., and Mitchell, J. K., 2001. Paleoliquefaction Studies in Continental Settings: Geologic and Geotechnical Factors in Interpretations and Back-Analysis, *Open-File Rep./U.S. Geol. Surv. 01-29*.

- Olson, S. M., Obermeier, S. F., and Stark, T. D., 2001. Interpretation of penetration resistance for back-analysis at sites of previous liquefaction, *Seismol. Res. Lett.* **72** (1), 46–59.
- Pond, E. C., and Martin, J. R., 1997. Estimated magnitudes and accelerations associated with prehistoric earthquakes in the Wabash Valley region of the central United States, *Seismol. Res. Lett.* **68** (4), 611–623.
- Robertson, P. K., and Wride, C. E., 1997. Cyclic Liquefaction and its Evaluation Based on the SPT and CPT, *Proceedings of NCEER Workshop on Evaluation of Liquefaction Resistance of Soils*, Salt Lake City, Utah, Jan. 5–6, 1996.
- Robertson, P. K., and Wride, C. E., 1998. Evaluating cyclic liquefaction potential using the cone penetration test, *Can. Geotech. J.* **35** (3), 442–459.
- Schmertmann, J. H., 1987. Discussion of “Time-dependent strength gain in freshly deposited or densified sand,” by James K. Mitchell, and Zoltan V. Solymar, *J. Geotech. Eng.* **113** (2), 173–175.
- Schmertmann, J. H., 1991. The mechanical aging of soils, The 25th Terzaghi Lecture, *J. Geotech. Eng.* **117** (9), 1288–1330.
- Seed, R. B., Cetin, K. O., Moss, R. E. S., Kammerer, A. M., Wu, J., Pestana, J. M., and Riemer, M. F., 2001. Recent advances in soil liquefaction engineering and seismic site response evaluation, *Proceedings of 4th Int. Conf. on Recent Advances in Geotech. Earthquake Eng. Soil Dyn.*, Paper No. SPL-2.
- Seed, H. B., and Idriss, I. M., 1971. Simplified procedure for evaluating soil liquefaction potential, *J. Soil Mech. Found. Div.* **97** (9), 1249–1273.
- Seed, H. B., Tokimatsu, K., Harder, L. F., and Chung, R. M., 1985. The influence of SPT procedures in soil liquefaction resistance evaluations, *J. Geotech. Eng.* **111** (12), 1425–1445.
- Skempton, A. W., 1986. Standard penetration test procedures and the effects in sands of overburden pressure, relative density, particle size, aging and overconsolidation, *Geotechnique*, London, **36** (3), 425–447.
- Stark, D., Obermeier, S. F., Newman, E. J., and Stark, J. M., 2002. Interpretation of ground shaking from paleoliquefaction features; <http://erp-web.er.usgs.gov/reports/annsum/vol43/cu/g0030.pdf>, (2/08/03)
- Talwani, P., and Schaeffer, W. T., 2001. Recurrence rates of large earthquakes in the South Carolina Coastal Plain based on paleoliquefaction data, *J. Geophys. Res.* **106** (B4), 6621–6642.
- Tuttle, M. P., Schweig, E. S., Sims, J. D., Lafferty, R. H., Wolf, L. W., Haynes, M. L., 2002. The earthquake potential of the New Madrid Seismic Zone, *Bull. Seismol. Soc. Am.* **92**, 2080–2089.
- Youd, T. L., and Garris, C. T., 1995. Liquefaction-induced ground-surface disruption, *J. Geotech. Eng.* **121** (11), 805–809.
- Youd, T. L., and Hoose, S. N., 1977. Liquefaction susceptibility and geologic setting, *Proceedings of 6th World Conference on Earthquake Engineering, New Delhi, India*, vol. 6, 37–42.
- Youd, T. L., and Idriss, I. M. (eds.), 1997. Summary Report, *Proceedings NCEER Workshop on Evaluation of Liquefaction Resistance of Soils, Tech. Rep. NCEER-97-0022*, edited by T. L. Youd and I. M. Idriss, National Center for Earthquake Engineering Research, Buffalo, pp. 1–40.

Youd, T. L., Idriss, I. M., Andrus, R. D., Arango, I., Castro, G., Christian, J. T., Dobry, R., Finn, W. D. L., Harder, L. F., Jr., Hynes, M. E., Ishihara, K., Koester, J. P., Liao, S. S. C., Marcuson, W. F., III, Martin, G. R., Mitchell, J. K., Moriwaki, Y., Power, M. S., Robertson, P. K., Seed, R. B., Stokoe, K. H., II, 2001. Liquefaction resistance of soils: Summary report from the 1996 NCEER and 1998 NCEER/NSF workshops on evaluation of liquefaction resistance of soils, *J. Geotech. Geoenviron. Eng.* **127** (10), 817–833.

(Received 19 January 2004; accepted 2 October 2004)